Crossover from space-charge-limited to recombination-limited transport in polymer light-emitting diodes

H. C. F. Martens,* W. F. Pasveer, and H. B. Brom
Kamerlingh Onnes Laboratory, Leiden University, P.O. Box 9504, 2300 RA Leiden, The Netherlands

J. N. Huiberts
Philips Research Laboratories, Professor Holstlaan 4, 5656 AA Eindhoven, The Netherlands

P. W. M. Blom
Materials Science Centre, University of Groningen, Nijenborgh 4, 9747 AG Groningen, The Netherlands
(Received 6 September 2000; published 13 March 2001)

By performing admittance spectroscopy as a function of frequency on polymer light-emitting diodes, inductive and capacitive charge-relaxation processes with different characteristic time scales are separated. The inductive contributions arise from the finite transit time of injected carriers, while the capacitive contributions stem from dielectric redistribution of charge density in the device. The crossover from inductive charge relaxation at low bias to capacitive charge relaxation at high bias marks the transition from space-charge-limited to recombination-limited current flow. This unexpected result shows that, while the individual carrier mobilities are strongly enhanced by the applied field, the recombination mobility remains unaffected.

DOI: 10.1103/PhysRevB.63.125328 PACS number(s): 72.80.Le, 73.61.Ph, 85.60.Jb

I. INTRODUCTION

Since the first report of electroluminescence in semiconducting conjugated polymers,[1,2] the potential applications of polymer light-emitting diodes (PLED's) have attracted widespread attention. The principal advantage of these materials is the combination of low-cost processing and mechanical flexibility, which allows for cheap and flexible displays.[1,2] As a result of the high external conversion efficiency, greater than 1% photon/carrier, attention has been focused especially on poly(p-phenylene vinylene), PPV, and its derivatives. At present, the performance of PLED's already meets many of the qualifications required for commercial applications. An overview of the current scientific and technological knowledge of PPV-based LED's can be found in Ref. 3.

Understanding charge transport in semiconducting PPV has been one of the major goals in the effort to optimize PLED operation. It has been demonstrated that transport in PPV-based hole-only devices is bulk space-charge limited.[4] For single-carrier space-charge-limited (SCL) transport the current-density–voltage $J(V)$ characteristic for a field-independent mobility is given by the famous Mott-Gurney square law

$$J=\frac{9}{8}\varepsilon_0\varepsilon\mu\frac{V^2}{L^3}, \tag{1}$$

with ε_0 the permittivity of free space, ε the relative dielectric constant, μ the mobility, V the applied voltage, and L the thickness. Experiments at high bias[5] have revealed that, apart from space-charge effects, a field-dependent hole mobility must be taken into account to understand the $J(V)$ characteristics. In PPV the hole mobility is well described by the empirical relation

$$\mu=\mu_0\exp(\gamma\sqrt{E}), \tag{2}$$

with μ_0 the zero-field mobility and γ the ''field-activation'' factor. This functional dependence, which appears generic for a large class of disordered organic semiconductors such as molecularly doped polymers, pendent group polymers, organic glasses, and conjugated polymers, has been confirmed by a wide variety of experimental techniques: time of flight,[6–13] current-voltage,[5,13,14] and admittance.[15,16] The specific $\sqrt{E}$ dependence of $\ln(\mu)$ arises from hopping transport in an energetically and spatially disordered system.[17–19] The current through electron-only devices of our material is three orders of magnitude below the hole current and exhibits a stronger field dependence, reminiscent of traps.[4] Such electron traps may result from contamination during processing. In a recent experiment, Bozano *et al.* reported a higher electron current in MEH-PPV [poly(2-methoxy),5-(2'-ethylhetoxy]-p-phenylene vinylene, which was analyzed in terms of a trap-free space-charge-limited current.[20] The derived electron mobility is also well described by the empirical $\sqrt{E}$ law, Eq. (2), but is an order of magnitude smaller than the hole mobility and exhibits stronger field dependence.

Admittance spectroscopy is a powerful tool to study charge-transport dynamics in solid state devices,[21] and has often been applied to study PLED's.[15,16,22–25] In general, charge transport processes that occur on time scale τ are reflected in the frequency-dependent electrical response around $\omega\sim\tau^{-1}$. For example, the transit of holes in PPV-based hole-only devices shows up as an inductive contribution to the complex admittance,[15] which provides an easy way to extract the transit time of injected holes, and hence the hole mobility, from these data.[15]

Here we apply admittance spectroscopy to investigate the charge-carrier dynamics in PPV-based LED's. In a preliminary study we pointed out that inductive contributions are present also in the PLED's, from which both the electron and hole mobility can be derived.[16] In the present work we extend this study, and demonstrate that in PLED's the presence

of both electrons and holes leads to a much richer behavior as compared to single-carrier devices. This allows us to elucidate the physical picture of the transport and recombination of electrons and holes through PPV-based LED's.

This paper is organized as follows. Experimental methods are outlined in Sec. II. In Sec. III we present the frequency-dependent response of the device, and indicate the different relaxation processes present in the device. Based on this analysis we introduce a bias-dependent equivalent-circuit model for the PLED that satisfactorily describes the experimental data in the frequency range (hertz to megahertz) and bias range (0–10 V) studied here. The ac response as a function of bias is discussed in Sec. IV. At low bias, inductive contributions due to hole and electron transit are clearly distinguished, yielding the respective carrier mobilities. At high bias, capacitive relaxation processes, due to charge redistribution in the electron-hole plasma, govern the frequency-dependent response. The evolution of the frequency-dependent response with bias reflects a crossover from space-charge-limited to recombination-limited current flow. We argue that this transition shows that the recombination efficiency in PLED's is not increased by the field-enhanced carrier mobilities.

II. EXPERIMENT

The devices studied consist of a thin layer of OC_1C_{10}-PPV (Refs. 26,27) sandwiched between two electrodes on top of a glass substrate. The polymer is spin coated on top of an optically transparent indium tin oxide (ITO) electrode. The high work function of ITO makes it suitable for hole injection. As the top electrode evaporated Ca is used, which has a low work function and serves as the electron injector. The different work functions of the anode and cathode give rise to a built-in voltage $V_{bi}=1.7$ V. The thickness of the devices studied here is $L=200$ nm; the active area of the diodes is typically $A=10-20$ mm^2.

Admittance measurements in the range of 5 Hz to 1 MHz are performed under a nitrogen atmosphere using a HP4192A impedance analyzer. The analyzer can superimpose a bias voltage from -35 V to 35 V on top of the ac voltage v_{ac}. The experimental results were checked to be independent of oscillator level ($v_{ac}=10-100$ mV). The complex admittance Y is defined as the ratio of ac current and ac voltage:

$$Y=i_{ac}/v_{ac}=G+iB=G+i\omega C, \tag{3}$$

with G the conductance, B the susceptance, C the capacitance, $i=\sqrt{-1}$, and $\omega=2\pi f$ the angular frequency. The real part of Y stems from the Ohmic current (in phase), while the imaginary part of Y reflects the displacement current (out of phase). In the present work we focus only on the imaginary part of the admittance, which most clearly reveals the different relaxation processes present in the PLED's. However, the fits to the proposed equivalent-circuit models were in all cases checked to be consistent with both the real and imaginary parts of Y.

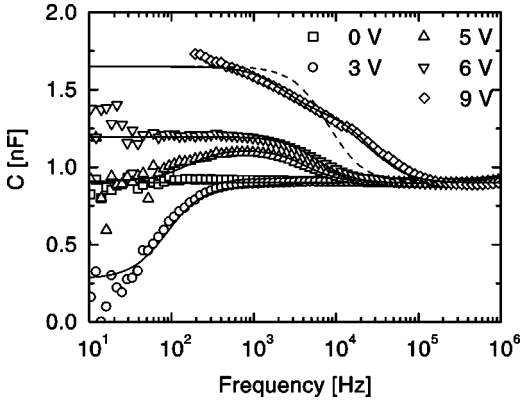

FIG. 1. Frequency-dependent capacitance of a polymer LED as a function of bias voltage. At zero bias the capacitance is nearly frequency independent. At low bias voltage a negative contribution to C sets in. In addition, at higher bias a positive contribution appears. This positive contribution dominates the frequency-dependent response at the highest bias voltages. Drawn lines are fits to equivalent-circuit models discussed in the text.

III. FREQUENCY DEPENDENT RESPONSE OF PLED'S

In Fig. 1 the frequency-dependent capacitance of a PLED ($L=200$ nm) is shown as a function of (forward) bias voltage. At zero bias C is essentially frequency independent and equals the geometrical capacitance $C_0=\varepsilon\varepsilon_0 A/L$ (ε_0 is the vacuum permittivity, $\varepsilon\approx 2$ the relative dielectric constant of the polymer). At low bias a negative contribution to C appears. Upon increasing V a positive contribution sets in, and this dominates the response at the highest bias. These contributions to C are more clearly visualized by plotting the differential susceptance $\Delta B=\omega(C-C_0)$. Figure 2 displays $-\Delta B$ at low bias. For comparison we include $-\Delta B$ for a hole-only device with similar thickness L and average electric field $E=(V-V_{bi})/L$. While in the hole-only device only a single relaxation peak is present, for the PLED two peaks can be distinguished. Apparently, at low bias two inductive (negative capacitance) contributions are present in the

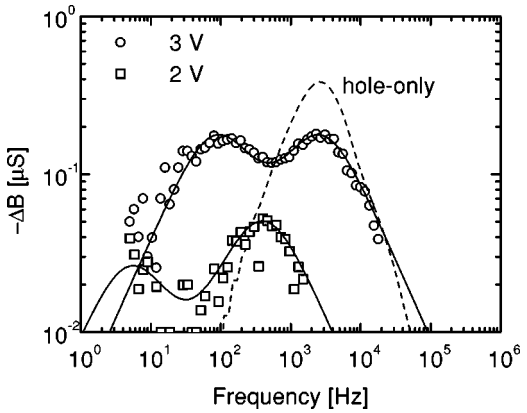

FIG. 2. Plot of the negative differential susceptance $-\Delta B=-\omega(C-C_0)$, for the data shown in Fig. 1. Two relaxation peaks are clearly distinguished. For comparison $-\Delta B$ of a hole-only device is shown (dashed line), revealing only a single relaxation peak. Solid lines are fits to the equivalent circuit shown in Fig. 4 below.

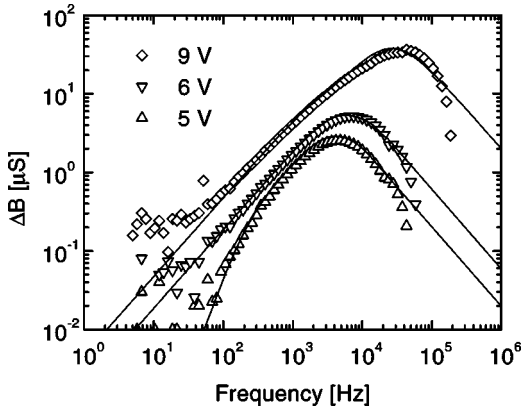

FIG. 3. Positive differential susceptance $\Delta B=\omega(C-C_0)$ for the data shown in Fig. 1. A single, capacitive relaxation time is observed. Solid lines are fits to the data, using the proposed equivalent-circuit model (see Fig. 4 below).

PLED. The behavior at high bias is shown in Fig. 3, revealing a single capacitive peak. Comparable relaxation peaks are not observed in hole-only devices.

Based on the above results we propose the empirical equivalent circuits shown in Fig. 4 to model the frequency-dependent response of the PLED for different bias regimes. The bulk resistance and capacitance of the device are given by R_B and C_B, respectively. The two inductive processes present at low bias are modeled by the R_1+L_1 series and R_2+L_2 series, which are both parallel to the bulk. In the intermediate bias regime, 4–6 V, one inductive contribution remains and a capacitive contribution R_3+C_3 appears. At the highest bias, only capacitive processes govern the response, and the device is modeled by taking two capacitive branches parallel to the bulk. Using this bias-dependent empirical model we can obtain excellent fits of our data; see Figs. 1, 2, and 3. At the highest bias, only a single capacitive relaxation peak is observed; see Fig. 3. However, taking only a single capacitive contribution when fitting $C(\omega)$ at high bias gives a large discrepancy; see the dashed line in Fig. 1. By taking an additional capacitive contribution (solid line) into account, the high-bias data are also reasonably well reproduced. From the fits we can derive the corresponding relaxation times of the different processes: $\tau_1=L_1/R_1$, $\tau_2=L_2/R_2$, and $\tau_3=R_3C_3$ (note that $\tau^{-1}=\omega_r$ corresponds to the peak position of ΔB). Unfortunately, τ_4 could not be very accurately determined from the present data. The derived relaxation times are plotted in Fig. 5 as a function of bias. Upon increasing the bias voltage the relaxation processes in the PLED become faster.

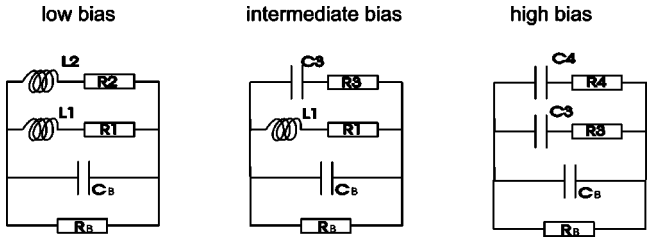

FIG. 4. Equivalent-circuit models to describe the bias-dependent complex admittance of our polymer LED's. At low bias (<4 V) two inductive charge-relaxation processes govern the response of the PLED. For intermediate bias (4–7 V) one inductive and one capacitive relaxation process are present in the device. At high bias (>7 V) two capacitive processes appear to govern the response. The inductive relaxation times of the circuits are $\tau_1=L_1/R_1$ and $\tau_2=L_2/R_2$. The capacitive relaxation times are given by $\tau_3=R_3C_3$ and $\tau_4=R_4C_4$.

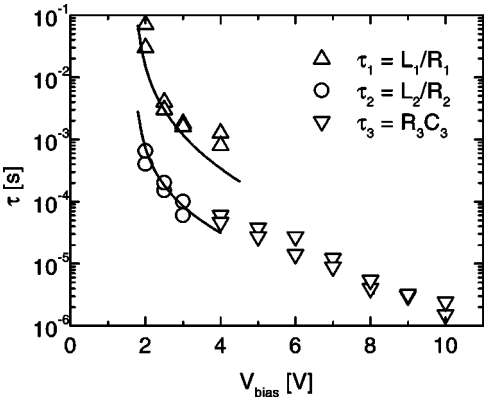

FIG. 5. Derived relaxation times of the charge-relaxation processes in a polymer LED. The values of τ_1 and τ_2 correspond to hole and electron transit times in the device, respectively. The third and fourth relaxation processes correspond to the redistribution of electrons and holes in the device; the data sets do not allow an accurate estimate of τ_4.

IV. MODELING AND DISCUSSION

A. Single-carrier devices

Neglecting possible contact constraints, single-carrier transport through an insulator is always space-charge limited, and the magnitude of the current is solely determined by the mobility, or equivalently by the transit time $\tau_t=L^2/(\mu V)$. The dotted line in Fig. 2 shows that the ac response of a hole-only device is of inductive nature. Hole transport in PPV is space-charge limited,[4] and it has been demonstrated that this gives rise to the inductive response.[15] In a SCL device, application of an ac voltage on top of a bias field leads to (time-dependent) injection of additional space charge. Under the influence of the bias field, the injected charge moves into the device to relax to the equilibrium space-charge distribution. Due to the finite transit time of injected charges, the corresponding current lags behind the ac voltage, and this gives an inductive contribution to the capacitance; see Eq. (3). For times short compared to τ_t, or frequencies $\omega>\tau_t^{-1}$, the injected carrier density cannot relax and the inductive contribution disappears. For single-carrier SCL devices the admittance can be exactly calculated.[15] It follows that the maximum of the inductive relaxation peak $\omega_r\approx 3.4\times\tau_t^{-1}$, with $\tau_t=L^2/(\mu V)$. The relaxation time of the space-charge density is $\tau=0.29\times\tau_t$. The factor 0.29 is a consequence of the nonhomogeneous field distribution in the device; for a homogeneous field distribution the relaxation peak would be located at $\omega_r=\tau_t^{-1}$. Charge transport in PPV is dispersive,[28] which is due to the

strongly disordered structure of the material. As a result the transit times of individual charge carriers exhibit a broad distribution. Although the distribution in transit times broadens the inductive contribution in PPV-based hole-only devices, the position of the relaxation peak, reflecting the ''average'' transit time, is not affected and still relates to the dc mobility.[15]

B. Double-injection devices

In a double-injection device, charge transport is governed not only by space-charge effects, but by the recombination efficiency of electrons and holes as well. The interplay between carrier transit time τ_t and recombination time τ_r determines the spatial distribution of electrons and holes in the device. Depending on the relative recombination strength, the current flow is either space-charge limited, recombination limited, or a combination of both.[29]

Charge transport in our PLED's falls into the class of the so-called bimolecular-recombination plasma.[29] An analytical solution of this problem has been obtained by Parmenter and Ruppel.[29] The relevant parameters in their work are the recombination mobility μ_r and normalized electron and hole mobilities ν_n and ν_p given by

$$\mu_r = \varepsilon\varepsilon_0 B/2q, \tag{4}$$

$$\nu_n = \mu_n/\mu_r, \tag{5}$$

$$\nu_p = \mu_p/\mu_r, \tag{6}$$

with q the electronic charge and B the bimolecular recombination constant. The use of the carrier and recombination mobility is for mathematical convenience; this is of course equivalent to a comparison of transit and recombination times. For the bimolecular-recombination plasma the current-density–voltage characteristic can be written as a Mott-Gurney square law, Eq. (1), with an effective mobility μ_{eff} given by[29]

$$\mu_{\text{eff}} = \tfrac{4}{9}\,\mu_r \nu_n \nu_p \left[\frac{\Gamma(\tfrac{3}{2}\,\nu_n + \tfrac{3}{2}\,\nu_p)}{\Gamma(\tfrac{3}{2}\,\nu_n)\Gamma(\tfrac{3}{2}\,\nu_n)}\right]^2 \left[\frac{\Gamma(\nu_n)\Gamma(\nu_n)}{\Gamma(\nu_n+\nu_p)}\right]^3, \tag{7}$$

where $\Gamma(x)$ represents the Euler gamma function.

It is instructive to consider the limits of strong and weak recombination. For these cases we schematically indicate in Fig. 6 the electron distribution (n) and hole distribution (p) throughout the device. For strong recombination, $\nu_n, \nu_p \ll 1$ (or $\tau_r \ll \tau_t$), the injected electrons and holes completely annihilate at the plane where they meet in the device. This case is shown on the left hand side of Fig. 6. The effective mobility simplifies to $\mu_{\text{eff}} = \mu_n + \mu_p$; the total current is in magnitude the same as the sum of the two single-carrier space-charge-limited currents that would run through the device in the absence of each other [see Eq. (1)]. For weak recombination, $\nu_n, \nu_p \gg 1$ (or $\tau_r \gg \tau_t$), both electrons and holes fully penetrate the device, the so-called plasma limit. The carrier

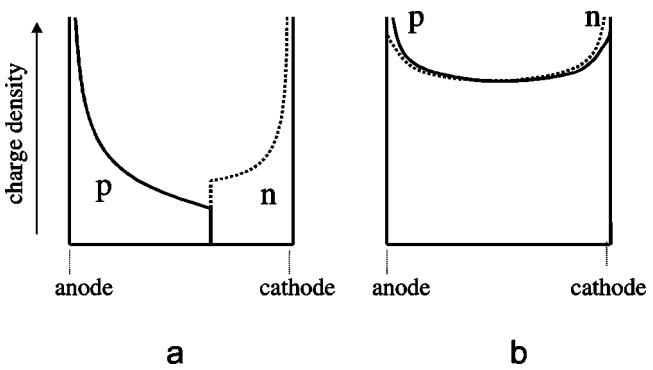

FIG. 6. Schematic distribution of electron density (n) and hole density (p) in a double-injection device. On the left is shown the case of strong recombination (infinite recombination constant). Where the opposite carriers meet they totally annihilate each other. Both the electron current J_n and hole current J_p are space-charge limited. The right hand side shows the case of weak recombination. Both electrons and holes flow through the entire device. Due to the mutual neutralization of electrons and holes, the current is recombination instead of space-charge limited.

densities for this case are schematically depicted in the right hand side of Fig. 6. In the plasma limit, the current is no longer limited by the accumulation of space charge, but by the loss of carriers through recombination. Due to mutual neutralization, the separate electron and hole densities are much larger than in a SCL device, and therefore the current significantly exceeds the single-carrier currents; in the absence of any recombination it would even be infinite. For weak recombination, the effective mobility, Eq. (7), simplifies to $\mu_{\text{eff}} = \frac{2}{3}\sqrt{2\pi\mu_n\mu_p(\mu_n+\mu_p)/\mu_r}$.

Which mechanism will limit current flow in PPV-based double-injection devices? The capture of oppositely charged carriers in PPV has been shown to be of the Langevin type.[32] The Langevin mechanism implies that the recombination efficiency is limited by the diffusion of electrons and holes toward each other in their mutual Coulomb field. The bimolecular recombination constant for this case is given by $B = (q/\varepsilon_0\varepsilon)(\mu_n+\mu_p)$. Hence the effective electron and hole mobilities simplify to $\nu_n = 2\mu_n/(\mu_n+\mu_p)$ and $\nu_p = 2\mu_p/(\mu_n+\mu_p)$. Since holes in PPV are much more mobile than electrons, $\mu_p \gg \mu_n$,[4,16] we expect $\nu_p \approx 2$ and $\nu_n \ll 1$. The effective mobility, Eq. (7), simplifies to $\mu_{\text{eff}} = \mu_p$ and the current is essentially a hole-only SCL current.

At low bias the ac response of the PLED's reveals inductive contributions (see Figs. 1 and 2), indeed indicating that the current is governed by space-charge effects. Since for SCL transport in a double-injection device the transit times of both electrons and holes determine the charge distributions, the presence of two inductive peaks in the PLED's (see Fig. 2), reflects the different transport dynamics of electrons and holes in the device.[16] Using $\tau = 0.29\tau_t$ and the field-dependent mobility, Eq. (2), the relaxation times τ_1 and τ_2 can be fitted (see the solid lines in Fig. 5). This gives for the hole mobility $\mu_0 = 3\times10^{-11}$ m^2/V s and $\gamma = 5\times10^{-4}$ (m/V)$^{1/2}$. For the electron mobility we find $\mu_0 = 3\times10^{-13}$ m^2/V s and $\gamma = 8\times10^{-4}$ (m/V)$^{1/2}$. These values are in good agreement with previously reported electron and

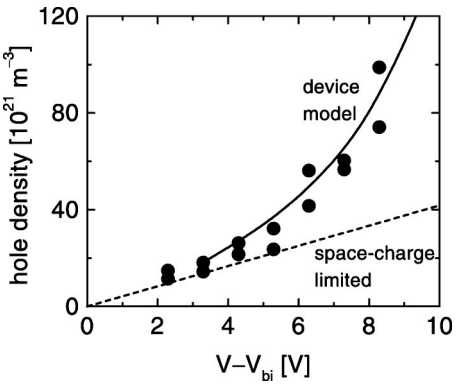

FIG. 7. Hole density in the PLED as a function of bias derived from the dielectric relaxation time τ_3 (see text). The experimentally derived data (dots) are in good agreement with the solid line representing the average hole density calculated using our device model (Refs. 19,30). The dashed line represents the carrier density for a space-charge-limited device, which lies significantly below the experimental results. In order to obey Poisson's equation, this implies that (partial) neutralization by injected electrons must occur, i.e., an electron-hole plasma must be present.

hole mobilities in these materials.[5,11–16,20] The results show that, if current is space-charge limited, admittance spectroscopy provides a tool to study the electron and hole mobility in double-injection devices; a more elaborate discussion can be found in Ref. 16. Especially for PPV, where, due to trapping, the intrinsic electron mobility cannot be easily derived from standard approaches such as time-of-flight[10,12] or current-voltage experiments,[4] this may prove valuable.

In the intermediate bias regime, 4–7 V, the inductive relaxation due to hole transit is no longer observed, and a capacitive contribution appears instead (see Figs. 1 and 3). The inductive contribution of the electrons persists but becomes less pronounced for increasing bias. At even higher bias, the inductive contributions have completely disappeared and the response has become fully capacitive (see Fig. 1). The suppression of the inductive processes reflects the fact that for higher bias the current is no longer space-charge limited. A capacitive response is expected for transport in the quasineutral plasma limit. The electron and hole densities in the device are so high that injected charges are equilibrated by the displacement of the holes and electrons in the plasma before they can transit the device. The rate at which that occurs is determined by the dielectric relaxation time of the plasma, τ_d, which is the time necessary for the reestablishment of quasineutrality after charge has been injected. The relaxation toward neutrality in the electron-hole plasma is governed by $\partial\rho/\partial t = -(\rho/\tau_d)$ (ρ is the carrier density), which shows that dielectric relaxation current indeed gives a capacitive response. The dielectric relaxation time relates to the plasma mobility μ and plasma carrier density ρ as

$$\tau_d = \frac{\varepsilon_0 \varepsilon}{q \rho \mu}. \tag{8}$$

The dielectric relaxation of the plasma involves the displacement of both electrons and holes; hence μ and ρ may depend in a nontrivial way on the respective mobilities and carrier densities. However, as shown above, the mobility of holes is 1–2 orders of magnitude higher than that of electrons, and it seems reasonable to assume that on short time scales (high frequencies) the dielectric relaxation is dominated by the movement of holes in the plasma. Taking $\mu = \mu_p$ we can estimate, using Eq. (8), the average hole density in the plasma from the τ_3 data. In Fig. 7 we present the hole density (dots) as a function of bias. The solid line represents the hole density calculated using our device model,[19,30] while the dashed line gives the hole density for the space-charge-limited regime. The derived hole density increases steeply with bias and, despite the crudeness of our analysis, is in good agreement with the model calculations. At high bias, the hole density in the PLED exceeds that for the space-charge-limited regime by a factor of 2. In order to satisfy Poisson's equation, electrons must be present to neutralize the positively charged holes, i.e., these results bear out our argument for the presence of an electron-hole plasma in PLED's at high bias.

C. Space-charge-limited and recombination-limited transport

According to Lampert and Mark[29] in a bimolecular-recombination insulator (which applies to PPV) the functional dependencies of the electron, hole, and field distributions on position are independent of the applied voltage: the limiting mechanism (space charge or recombination) for current flow is independent of the applied electrical field. However, in our PLED's a change in current-limiting mechanism does occur with increasing bias. As it is not expected that a different recombination mechanism takes over at high bias, this is a surprising result. The mechanism of current flow through the bimolecular-recombination plasma is fully determined by the values of ν_n and ν_p, Eqs. (5) and (6). Therefore, to understand this result, we must consider the bias dependence of ν_n and ν_p.

In PLED's, recombination is of the Langevin type for which the bimolecular-recombination constant is given by the sum of the carrier mobilities. The application of an electrical field considerably enhances the individual carrier mobilities. However, whether this also enhances the bimolecular recombination[31] or not[32] is not clear. Using the electron and hole mobilities derived above, we can calculate the normalized mobilities for these two cases; see Fig. 8. The solid lines represent the case of field-independent recombination: $B = (q/\varepsilon_0\varepsilon)[\mu_n(E=0) + \mu_p(E=0)]$. Since B is just a constant, both ν_n and ν_p increase strongly with increasing bias due to the exponential dependence of the electron and hole mobilities on $\sqrt{E}$. The dotted lines show ν_n and ν_p in the case that the recombination is enhanced by the field-dependent mobilities given by Eq. (2): $B(E) = (q/\varepsilon_0\varepsilon)[\mu_n(E) + \mu_p(E)]$. As $\mu_p \gg \mu_n$, the field dependence of the bimolecular-recombination constant B closely follows the field dependence of μ_p in this case, which explains the near field independence of the normalized hole mobility [see Eq. (6)]. Since the electron transport exhibits stronger field dependence compared to μ_p (and B), for field-dependent recombination ν_n also increases with bias, albeit

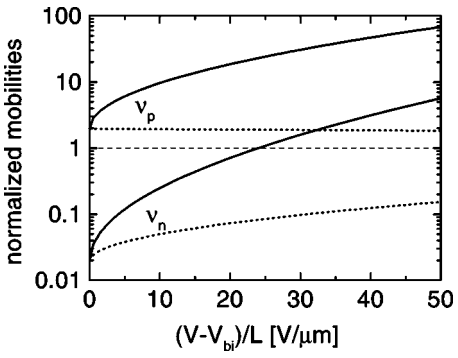

FIG. 8. Calculated normalized electron mobility ν_n and normalized hole mobility ν_p as a function of electrical field for the PPV-based LED's studied here. Solid lines represent the case of a field-independent recombination mechanism. Dotted lines represent the normalized mobilities for a field-enhanced recombination mechanism. Only when both ν_n and ν_p are larger than 1 will the current be recombination limited.

the increase is much less pronounced than in the case of field-independent recombination. The dashed horizontal line in Fig. 8 marks $\nu=1$.

At low bias, for both the field-dependent and the field-independent recombination mechanisms, $\nu_p>1$ and $\nu_n \ll 1$. In this regime the current is space-charge limited, which agrees with the inductive response of the devices observed in the admittance experiments. At high bias the response is capacative. This marks a crossover to recombination-limited transport, which occurs when both $\nu_n>1$ and $\nu_p>1$. It is evident from Fig. 8 that this happens only when a field-independent recombination mechanism is assumed (solid lines). If the recombination were enhanced by the field-dependent mobilities (dotted lines), only at very high fields >100 V/μm would a regime be reached in which both $\nu_n \approx 1$ and $\nu_p \approx 1$ and, apart from space charge, recombination effects would be important. By contrast, the admittance experiments clearly show that already around $V=7$ V ($E \approx 25$ V/μm) space-charge effects no longer dominate and instead an electron-hole plasma is formed. This experimental value for the crossover field is in excellent agreement with the field where $\nu_n=1$ for the case of the field-independent recombination mechanism.

Physically, the field independence of the recombination mechanism can be readily understood.[32] The application of a biasing electrical field enhances the movement of carriers toward each other along the potential gradient. However, the diffusion of carriers in directions perpendicular to the field is not enhanced and thus becomes the rate-limiting step in the recombination process at high fields. As a result the recombination efficiency is not enhanced by the field.

Finally, note that the formation of the electron-hole plasma implies a reduction of PLED efficiency since not all injected carriers recombine. Thus the crossover from the space-charge- to the recombination-limited regime is unwanted in applications like matrix displays under pulse operation where high drive voltages are used.

V. CONCLUSION

Admittance spectroscopy allows one to differentiate between the different transport processes in polymer LED's. At low bias the inductive response shows that transport in PLED's is governed by space-charge effects. This agrees with a Langevin recombination mechanism in combination with a large ratio of hole and electron mobilities in PPV, leading to a strong recombination efficiency. However, at high bias ($E>25$ V/μm) the capacitive response indicates the presence of an electron-hole plasma in our devices, implying that the recombination is relatively weak. This unexpected crossover from space-charge-limited to recombination-limited transport as a function of bias strongly indicates that, while the individual carrier mobilities strongly increase at high fields, the recombination mechanism is not enhanced by the biasing electrical field.

ACKNOWLEDGMENT

This research was sponsored by the Stichting Fundamenteel Onderzoek der Materie which is part of the Dutch Science Organization.

*Electronic address: martens@phys.leidenuniv.nl

[1] J.H. Burroughes, D.D.C. Bradley, A.R. Brown, R.N. Marks, K. Mackay, R.H. Friend, P.L. Burn, and A.B. Holmes, Nature (London) **347**, 539 (1990).

[2] D. Braun and A.J. Heeger, Appl. Phys. Lett. **58**, 1982 (1991).

[3] R.H. Friend, R.W. Gymer, A.B. Holmes, J.H. Burroughes, R.N. Marks, C. Taliani, D.D.C. Bradley, D.A. Dos Santos, J.L. Brédas, M. Lögdlung, and W.R. Salaneck, Nature (London) **397**, 121 (1999).

[4] P.W.M. Blom, M.J.M. de Jong, and J.J.M. Vleggaar, Appl. Phys. Lett. **68**, 3308 (1996).

[5] P.W.M. Blom, M.J.M. de Jong, and M.G. van Munster, Phys. Rev. B **55**, R656 (1997).

[6] D.M. Pai, J. Chem. Phys. **52**, 2285 (1970).

[7] W.D. Gill, J. Appl. Phys. **43**, 5033 (1972).

[8] L.B. Schein, A. Peled, and D. Glatz, J. Appl. Phys. **66**, 686 (1989).

[9] P.M. Borsenberger and D.S. Weiss, *Organic Photoreceptors for Imaging Systems* (Dekker, New York, 1993), Chap. 8, p. 181, and references therein.

[10] H. Meyer, D. Haarer, H. Naarmann, and H.H. Hörhold, Phys. Rev. B **52**, 2587 (1995).

[11] E. Lebedev, Th. Dittrich, V. Petrova-Koch, S. Karg, and W. Brütting, Appl. Phys. Lett. **71**, 2686 (1997).

[12] M. Redecker, D.D.C. Bradley, M. Inbasekaran, and E.P. Woo, Appl. Phys. Lett. **73**, 1565 (1998).

[13] I.H. Campbell, D.L. Smith, C.J. Neef, and J.P. Ferraris, Appl. Phys. Lett. **74**, 2809 (1999).

[14] H.C.F. Martens, P.W.M. Blom, and H.F.M. Schoo, Phys. Rev. B **61**, 7489 (2000).

[15] H.C.F. Martens, H.B. Brom, and P.W.M. Blom, Phys. Rev. B **60**, R8489 (1999).

[16] H.C.F. Martens, J.N. Huiberts, and P.W.M. Blom, Appl. Phys. Lett. **77**, 1852 (2000).

[17] H. Bässler, Phys. Status Solidi B **175**, 15 (1993).
[18] S.V. Novikov, D.H. Dunlap, V.M. Kenkre, P.E. Parris, and A.V. Vannikov, Phys. Rev. Lett. **81**, 4472 (1998).
[19] P.W.M. Blom and M.C.J.M. Vissenberg, Mater. Sci. Eng., R. **27**, 53 (2000).
[20] L. Bozano, S.A. Carter, J.C. Scott, G.G. Malliaras, and P.J. Brock, Appl. Phys. Lett. **74**, 1132 (1999).
[21] J.R. MacDonald, *Impedance Spectroscopy* (John Wiley & Sons, New York, 1987).
[22] M. Meier, S. Karg, and W. Riess, J. Appl. Phys. **82**, 1961 (1997).
[23] Y. Li, J. Gao, G. Yu, Y. Cao, and A.J. Heeger, Chem. Phys. Lett. **287**, 83 (1998).
[24] G. Yu, Y. Cao, C. Zhang, Y. Li, J. Gao, and A.J. Heeger, Appl. Phys. Lett. **73**, 111 (1998).
[25] S.H. Kim, K.-H. Choi, H.-M. Lee, D.-H. Hwang, L.-M. Do, H.Y. Chu, and T. Zyung, J. Appl. Phys. **87**, 882 (2000).
[26] D. Braun, E.G.J. Staring, R.C.J.E. Demandt, G.L.J. Rikken, Y.A.R.R. Kessener, and A.H.J. Venhuizen, Synth. Met. **66**, 75 (1994).
[27] C. Liedenbaum, Y. Croonen, P. van de Weijer, J. Vleggaar, and H. Schoo, Synth. Met. **91**, 109 (1997).
[28] P.W.M. Blom and M.C.J.M. Vissenberg, Phys. Rev. Lett. **80**, 3819 (1998).
[29] M.A. Lampert and P. Mark, *Current Injection in Solids* (Academic, New York, 1970).
[30] P.W.M. Blom and M.J.M. de Jong, IEEE J. Sel. Top. Quantum Electron. **4**, 105 (1998).
[31] D.J. Pinner, R.H. Friend, and N. Tessler, J. Appl. Phys. **86**, 5116 (1999).
[32] P.W.M. Blom, M.J.M. de Jong, and S. Breedijk, Appl. Phys. Lett. **71**, 930 (1997).